Synthesis, Chain Helicity, Assembling Structure, and Biological Compatibility of Poly(phenylacetylene)s Containing L-Alanine Moieties

Kevin K. L. Cheuk,[†] Bing Shi Li,[†,‡] Jacky W. Y. Lam,[†] Yong Xie,[§] and Ben Zhong Tang*[,†,⊥]

Departments of Chemistry and Biology, The Hong Kong University of Science & Technology (HKUST), Clear Water Bay, Kowloon, Hong Kong, China; Institute of Chemistry, Chinese Academy of Sciences, Beijing 100080, China; and Department of Polymer Science and Engineering, Zhejiang University, Hangzhou 310027, China

Received April 30, 2008; Revised Manuscript Received June 23, 2008

ABSTRACT: A functional phenylacetylene monomer containing a naturally occurring building block of L-alanine, namely 4-ethynylbenzoyl-L-alanine methyl ester (PA-Ae), was synthesized. The monomer was polymerized by organorhodium catalysts, giving the corresponding "polyester" (PPA-Ae) with high molecular weights (M_w up to 1.2×10^6) and stereoregularities (*Z* content up to 97%) in high yields (up to ~91%). The polyene backbone of PPA-Ae undergoes irreversible *Z*-to-*E* isomerization at ~180−250 °C. The ester groups in the pendants of the polymer are selectively deprotected by the base-catalyzed hydrolysis, producing a "polyacid" with "free" L-alanine pendants (PPA-A). While PA-Ae monomer is CD-inactive at wavelengths longer than 300 nm, both PPA-Ae and PPA-A polymers exhibit strong Cotton effects in the long wavelength region where their polyene backbones absorb, indicating that the chiral pendants have induced the polymer chain to take a helical conformation with an excess in one-handedness. Upon natural evaporation of its solutions, the amphiphilic chains of PPA-Ae self-associate in a cooperative fashion, furnishing a variety of organizational morphologies including twisting cables, spiral ribbons, spherical vesicles, and helical nanotubes. The polymers are biocompatible: the living cells are all survived after they have been subcultured in the presence of the polymers.

Introduction

Amino acids are the building blocks of proteins, which often take a helical chain conformation.[1] Our research groups have been interested in the integration of proteinogenic amino acids with conjugated polymers, in an effort to fabricate macromolecular wires with biological compatibility and optical and photonic activity.[2] We have succeeded in the design and synthesis of poly(phenylacetylene)s (PPAs) containing amino acid moieties, such as L-leucine methyl ester (PPA-Le) and its "free" acid form (PPA-L; Chart 1).[3] The asymmetric force field of the chiral amino acid pendants induces the polyacetylene backbones to spiral in a screw sense, resulting in the formation of helical polymer chains with an excess in one-handedness. In other words, the chirality of the L-leucine pendant has been transformed to the helicity of the PPA skeleton. Moreover, the amphiphilicity of the helical polymer chains enables them to self-assemble into biomimetic hierarchical structures,[2b,4] which are biologically compatible and may be used as scaffold materials for tissue engineering.

In our previous work, we have studied the effects of the "tails" attached to the ester groups and the "spacers" inserted between the PPA skeletons and the amino acid moieties on the chirality transcription processes from the stereogenic centers to the polymer backbones. It has been found that the attachment of an achiral alkyl tail to the ester group does not work to the benefit of the chirality transcription. For example, while the L-leucine-containing PPA bearing a long octyl tail (PPA-Lo; Chart 1) takes a helical chain conformation, its optical rotation and molar ellipticity values are both somewhat lower than those of its congener with a short methyl group (PPA-Le) measured under the identical conditions.[2e] Insertion of an achiral alkyl spacer between the PPA skeleton and the leucine moiety has proven detrimental. For example, the polymer containing a long decyl spacer (PPA-dLe; Chart 1) is practically optically inactive and circular dichroism (CD) silent.[3] Evidently, the flexible spacer of alkyl chain has shut down the chirality transcription process from the leucine moiety to the polymer backbone.

Chart 1

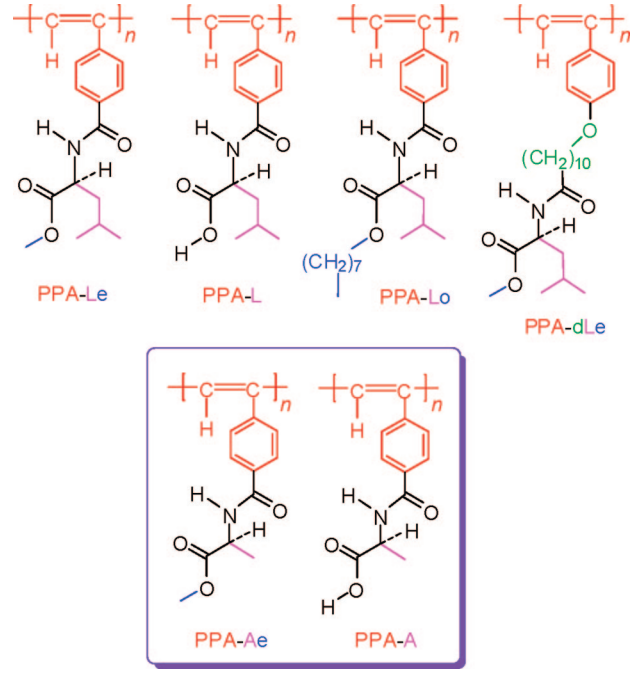

* Corresponding author: Ph +852-2358-7375; Fax +852-2358-1594; e-mail tangbenz@ust.hk.
† Department of Chemistry, HKUST.
‡ Chinese Academy of Sciences.
§ Department of Biology, HKUST.
⊥ Zhejiang University.

10.1021/ma800976e CCC: $40.75
Published on Web 07/23/2008

Scheme 1

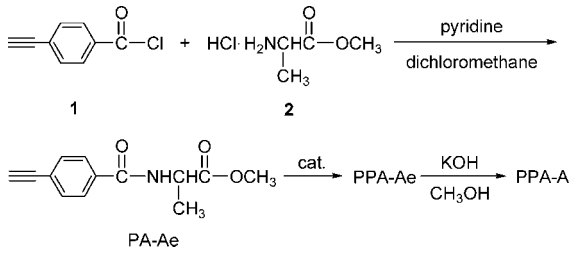

Table 1. Polymerization of PA-Ae Monomer[a]

no.	catalyst[b]	solvent[c]	yield (%)	M_w[d]	M_w/M_n[d]	Z (%)[e]
1	$[Rh(cod)Cl]_2$	THF	70.0	236 000	4.3	92.1
2	$[Rh(cod)Cl]_2$	THF/TEA	85.0	231 000	3.1	87.1
3	$[Rh(cod)Cl]_2$	DCM	34.0	219 000	4.4	93.8
4	$[Rh(cod)Cl]_2$	DCM/TEA	68.0	286 000	2.9	97.0
5	$[Rh(cod)Cl]_2$	dioxane	91.0	165 000	3.6	97.2
6	$[Rh(cod)Cl]_2$	toluene	81.0	57 000	5.4	91.6
7	$Rh(cod)(NH_3)Cl$	THF	89.0	354 000	7.8	91.9
8	$Rh(cod)(tos)(H_2O)$	THF	49.0	243 000	7.2	84.8
9	$Rh(cod)(tos)(H_2O)$	THF/TEA	35.0	293 000	3.8	89.7
10	$[Rh(nbd)Cl]_2$	THF	72.0	1 201 000	7.2	89.5
11	$[Rh(nbd)Cl]_2$	THF/TEA	83.0	426 000	5.1	78.3
12	$Rh(nbd)(tos)(H_2O)$	THF	32.0	246 000	3.5	94.3
13	$Rh(nbd)(tos)(H_2O)$	THF/TEA	91.0	337 000	7.0	89.5

[a] Carried out at room temperature in an atmosphere of nitrogen for 24 h; $[M]_0 = 0.1$ M, [cat.] = 5 mM. [b] Abbreviation: nbd = 2,5-norborndiene, cod = 1,5-cyclooctadiene, tos = *p*-toluenesulfonate, DCM = dichloromethane, TEA = triethylamine. [c] Volume of solvent used: 2 mL; volume of TEA added: 1 drop. [d] Estimated by gel permeation chromatography (GPC) in THF on the basis of a polystyrene calibration. [e] Determined by ^{1}H NMR analysis.

How will the bulkiness of the chiral group affect the chirality transcription? To answer this question, in this work, we replaced the "big" isobutyl group by a "small" methyl group, that is, changed L-leucine to L-alanine, which is the smallest in size among the 20 proteinogenic amino acids (except for achiral glycine). In this paper, we report the syntheses, structures, and properties of the PPA bearing L-alanine methyl ester pendants (PPA-Ae) and its free acid form (PPA-A; Chart 1).

Results and Discussion

Polymer Synthesis. We elaborated a single-step reaction route for the synthesis of PA-Ae monomer (Scheme 1). The amidation of 4-ethynylbenzoyl chloride (**1**) with L-alanine methyl ester (**2**) proceeded smoothly, giving a white solid of PA-Ae in ~68% yield. We characterized the monomer structure by spectroscopic methods and obtained satisfactory analysis data (see Experimental Section for details). Halides of tungsten and molybdenum are well-known catalysts for the polymerizations of substituted acetylenes[5] but none of them was capable of initiating the polymerizations of PA-Ae in either dioxane or toluene at 40 °C. Addition of a cocatalyst of tetraphenyltin or raising the polymerization temperature did not help. The catalysts might have been poisoned by the polar amino acid moiety of the monomer.

Since late-transition-metal complexes are more tolerant of functional groups,[6] we admixed PA-Ae with $[Rh(cod)Cl]_2$ in THF. After stirring at room temperature for 24 h, we obtained a high molecular weight polymer in a high yield (Table 1, no. 1). The polymer yield is further increased in the presence of triethylamine (TEA). A high molecular weight polymer is isolated from the reaction conducted in dichloromethane (DCM). The polymerization results are even better when a small amount of TEA is added. The reactions carried out in dioxane and toluene produce polymers in over 80% yields, but their molecular weights are relatively low. $Rh(cod)(NH_3)Cl$ and $Rh(cod)(tos)(H_2O)$ also function well for the polymerization, giving polymers with high molecular weights in good yields.

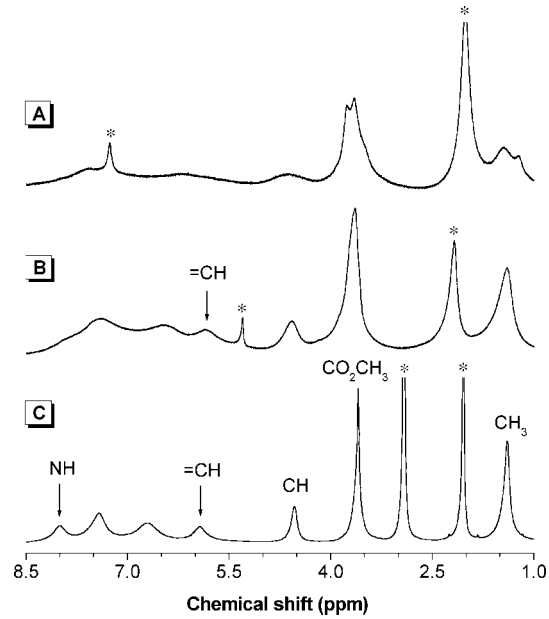

Figure 1. ^{1}H NMR spectra of (A) chloroform-*d*, (B) DCM-d_2, and (C) acetone-d_6 solutions of PPA-Ae (sample from Table 1, no. 11). The resonance peaks of the solvents and water are marked with asterisks.

Catalytic activities of organorhodium complexes with nbd ligand are also investigated. $[Rh(nbd)Cl]_2$ performs well, producing polymers with M_w's up to 1.2×10^6 in high yields. $Rh(nbd)(tos)(H_2O)$ works as an excellent catalyst in solvents mixed with TEA. For example, the polymer yield and molecular weight obtained in THF/TEA are respectively 3.8- and 1.4-fold higher than those prepared in THF alone.

Structural Characterization. The polymers were characterized by spectroscopic techniques, from which satisfactory analysis data were obtained (see Experimental Section). The monomer shows a C≡C stretching vibration band at ~2100 cm^{-1}, which is absent in the IR spectrum of the polymer. Although the ^{1}H NMR spectrum of PPA-Ae measured in chloroform-*d* is poorly resolved, there is no resonance peak associated with the ethynyl proton of PA-Ae at δ 3.2 (Figure 1A). The broad resonance peaks are probably due to the existence of multiple intra- and interchain hydrogen bonds in the polymer. The hydrogen bonds induce the polymer strands to aggregate and restrict the motions of their protons, which lengthen the relaxation times and broaden the resonance peaks.[7] The resonance peak of the dissolved water shifts from its general position at δ 1.56 to 2.0 due to its hydrogen bonding with the amino acid pendants of the polymer solute.

Better-resolved spectrum is obtained in DCM-d_2, where the resonance of the olefin proton of the polymer with a *Z*-s-*E* conformation is observed at δ 5.8.[8] The spectral quality is even better in acetone-d_6, allowing us to assign the resonance peaks and study the stereostructure of the polymer. Using an equation developed by our and other groups,[2,9] the *Z* content of PPA-Ae is calculated to be 78.3%. The polymers prepared under other conditions are all *Z*-rich (Table 1), agreeing with the early findings that organorhodium complexes generally produce polyacetylenes with *Z*-rich conformations.[10] Analysis by ^{13}C NMR spectroscopy confirms that the acetylenic triple bond of PA-Ae has been transformed into the olefinic double bond of PPA-Ae. The polymer shows no resonance peaks of the triple-bond carbons of PA-Ae at δ 82.7 and 79.6. On the other hand, new peaks associated with the resonances of the backbone olefin carbons are observed at δ 146.5 and 128.5.[11]

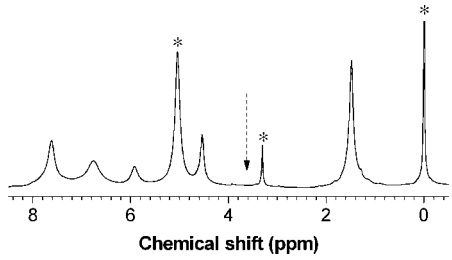

Figure 2. ^{1}H NMR spectrum of PPA-A in methanol-d_4 solution. The resonance peaks of TMS, solvents, and water are marked with asterisks.

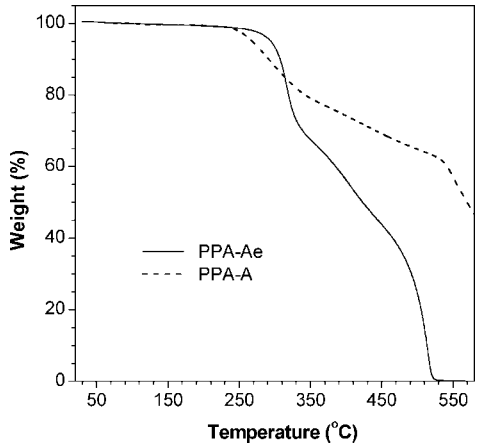

Figure 3. TGA thermograms of PPA-Ae (sample taken from Table 1, no. 11) and PPA-A measured under nitrogen at a heating rate of 20 °C/min.

Deprotective Hydrolysis. After the success in converting PA-Ae to PPA-Ae, we tried to cleave the methyl ester protecting groups and transform the "polyester" to its "polyacid" form (PPA-A). The deprotection reaction was carried out in methanol using KOH as cleaving agent.[12] After stirring for 1 h at room temperature, the polymer solution was poured into a dilute aqueous solution of hydrochloric acid, from which PPA-A was isolated in a high yield (∼96%).

^{1}H NMR spectroscopy was used to examine the structural integrity of the hydrolyzed product. The spectrum of PPA-A in methanol-d_4 shows no resonance peak of the methyl ester at δ 3.6 (Figure 2). Although the amide peak is not observed due to its exchange with the protic residue of the solvent,[7] the appearance of the proton resonance peaks at δ 5.9 (HC=), 4.5 (NHC*H*), and (CHCH_3) indicates that the hydrolysis reaction has proceeded to completion and has caused no harm to the polyene main chains and the amino acid pendants. The high selectivity of the ester deprotection reaction allows us to prepare polyacid with high structural homogeneity. The *Z* content of PPA-A is estimated to be 75.9%, parallel to that of its polyester parent (78.3%), revealing that stereoregularity of the polymer chain is virtually unaffected by the hydrolysis reaction.

Thermal Properties. "Polyester" PPA-Ae is soluble in common organic solvents such as chloroform, DCM, and THF, whereas its acid cousin PPA-A dissolves only in polar solvents such as methanol, DMF, and DMSO. Both polymers are thermally stable. Thermogravimetric analysis (TGA) reveals that PPA-Ae and PPA-A do not lose any weights when heated to a temperature as high as 270 °C (Figure 3). Their thermal stabilities are higher than that of their PPA parent, which degrades readily at 225 °C.[13] Hydrogen bonding between the amino acid pendants may have rigidified the polymer chains, enhancing their resistance to thermolysis.

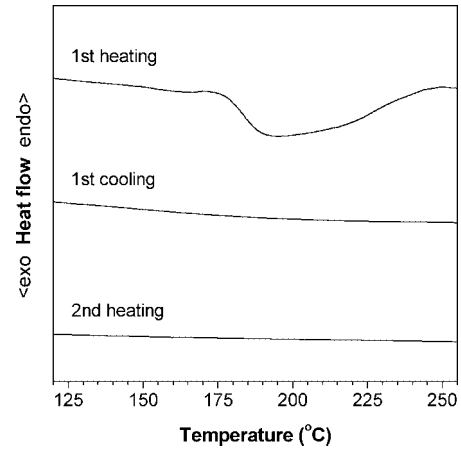

Figure 4. DSC thermograms of PPA-Ae (sample taken from Table 1, no. 11) recorded under nitrogen at a heating rate of 10 °C/min.

Table 2. Specific Optical Rotations of Monomer PA-Ae and Its Polymers PPA-Ae and PPA-A in Different Solvents

	$[\alpha]_D^{20}$, deg (*c*, g/dL)		
solvent	PA-Ae	PPA-Ae	PPA-A
chloroform	+35.5 (0.138)	−953.2 (0.044)	
DCM	+38.9 (3.525)	−624.1 (0.038)	
THF	+16.7 (0.150)	+440.0 (0.030)	
acetone		+642.6 (0.038)	
water[a]			+313.2 (0.038)
MeOH		+405.4 (0.064)	+300.0 (0.035)
DMF		+526.8 (0.041)	+315.6 (0.032)
DMSO			+391.4 (0.035)

[a] Alkalified with NaOH (0.2 M).

It is well-known that *Z*-rich polyacetylene undergoes irreversible *Z*-to-*E* isomerization upon thermal treatment.[14] The chain segments of PPA-Ae and PPA-A with *Z* conformation may also isomerize into *E* structure if a sufficient energy is supplied. Figure 4 shows the differential scanning calorimetry (DSC) curves of PPA-Ae recorded under nitrogen during the heating and cooling cycles. In the first heating scan, a broad exothermic peak in the temperature range of 175−250 °C is detected. Since PPA-Ae is thermally stable up to 270 °C, the exothermic valley at ∼200 °C is thus not due to the chain scission but associated with the *Z*-to-*E* isomerization. The successive first cooling and second heating cycles give only flat lines parallel to the abscissa, showing no peak at ∼200 °C. Thus, similar to its polyacetylene parent, the isomerization process of PPA-Ae is also irreversible.

Chain Helicity. To get some clues about whether the polyacetylene chains are induced to helically rotate by the "small" L-alanine pendants, we measured specific optical rotations ($[\alpha]_D^{20}$) of the polymers at 20 °C. The absolute $[\alpha]_D^{20}$ values of PPA-Ae are much higher than those of its monomer (up to ∼30-fold) in the same solvents (Table 2). It is known that a polymer chain with a helical conformation can exhibit very high optical activity.[15−17] The high $[\alpha]_D^{20}$ values of PPA-Ae suggest that its optical activity is not from its chiral amino acid pendants but from its helical polyacetylene strand or that the "small" L-alanine group has induced the polymer chain to spiral in a screw sense. Interestingly, the $[\alpha]_D^{20}$ value of PPA-Ae varies drastically with solvent. When the solvent is changed from chloroform to DCM to DMF, the $[\alpha]_D^{20}$ value of the polymer is changed in magnitude and/or sign from −953 to −624 to +527. Polyacid PPA-A displays similarly high $[\alpha]_D^{20}$ values in alkalified water, methanol, DMF, and DMSO. Because the polymer is insoluble in nonpolar solvents, we cannot measure its optical activities in the solvents with appreciably different polarizabilities.

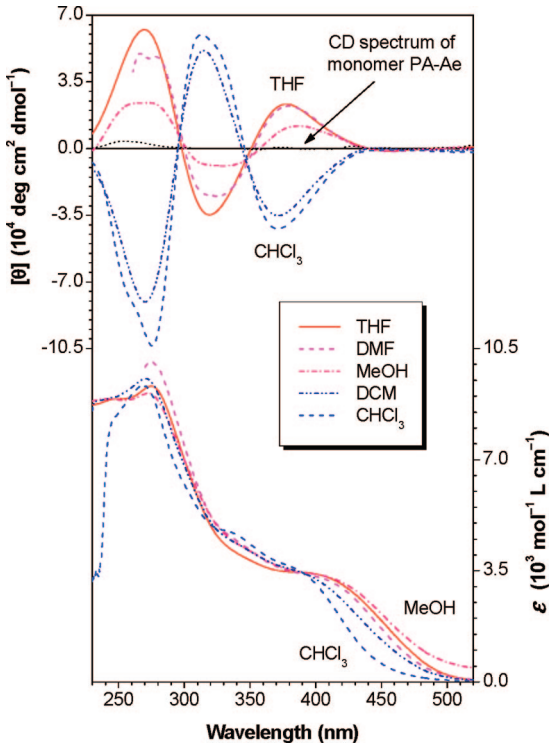

Figure 5. CD and UV spectra of PPA-Ae (sample taken from Table 1, no. 11) in different solvents. Polymer concentration (mM): ~1.5 (CD), 0.1−0.2 (UV). The CD spectrum of a chloroform solution of monomer PA-Ae with a similar concentration is shown for comparison. The spectral data in DMF below 260 nm were not taken to avoid the interference from the solvent absorption.

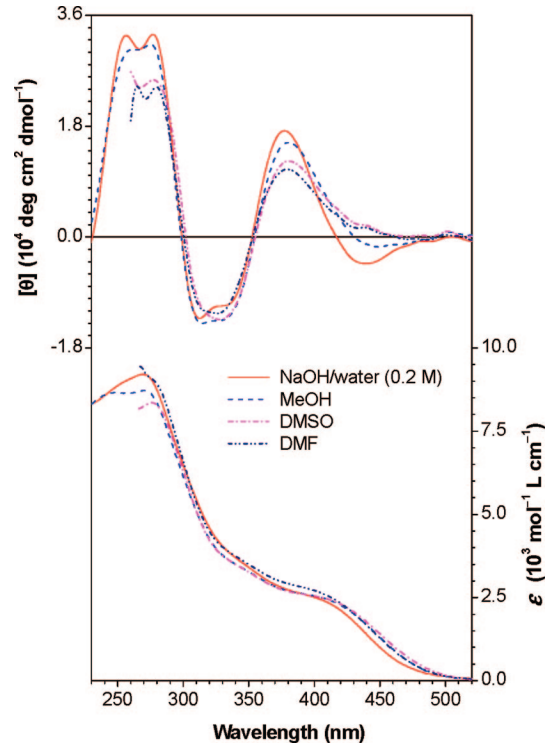

Figure 6. CD and UV spectra of PPA-A in different solvents. Polymer concentration (mM): ~1.5 (CD), 0.1−0.2 (UV). The spectral data in DMSO and DMF below 260 nm were not taken to avoid the interference from the solvent absorption.

The high $[\alpha]_D^{20}$ values of the polymers imply that their chain segments take a helical conformation. To confirm this, we conducted CD analysis, which is a powerful tool for studying helical structures.[18] The upper part of Figure 5 shows the CD spectra of PPA-Ae (polymer) in different solvents as well as PA-Ae (monomer) in chloroform. While the monomer is CD-inactive at wavelengths longer than 300 nm, strong Cotton effects associated with the absorptions of the polyene backbone are observed in the spectrum of PPA-Ae in chloroform at 310 and 372 nm. This ambiguously confirms that the polymer chain takes a helical conformation with a large excess in one-handedness. Like proteins, PPA-Ae changes its chain conformation with a change in the surrounding environment (or dissolving media).[19] When the solvent is changed from chloroform to DCM, the spectral profile remains almost unchanged but the peak intensity is weakened, implying that a fraction of the helical chain segments has reversed their screw sense. In THF, DMF, and methanol, the CD pattern of the polymer is completely inverted in sign, suggesting that the relative population of right- and left-handed helical chain segments is switched. While the intensity of the first Cotton effect in THF and DMF is similar, the ellipticity in methanol is 2 times lower.

The lower part of Figure 5 shows the absorption spectra of PPA-Ae in different solvents. In methanol, its polyene backbone absorbs at ~420 nm. Similar spectra are obtained in THF and DMF. When the solvent is changed to DCM and chloroform, the spectrum slightly blue-shifts. Overall, the UV spectrum of the polymer is less sensitive to the solvent change than its CD spectrum, indicating that CD is a more useful tool for probing conformational change of a helical macromolecule.

As mentioned above, polyacid PPA-A is only soluble in polar solvents, which significantly restricts our choice of solvents in the study of the solvent effect on its chiroptical properties. Since the solvents we used all have fairly similar polarities, no profound solvent effects on the UV spectra of the polyacid solutions are observed (lower panel of Figure 6). Whereas the conjugation of the PPA-A chain seems insensitive to the change in the solvent, its helicity varies with solvent to a greater extent. In DMF, the polymer shows a positive, first Cotton effect at 380 nm with a molar ellipticity of $\sim 1.0 \times 10^4$ deg cm^2 dmol^{-1}. When the solvent is changed to DMSO, methanol, and alkalified water, the CD band is located at a similar wavelength with no sign inversion but the peak becomes progressively stronger.

Helical conformation of a polymer chain can be induced by chiral pendants and stabilized by various covalent forces, especially hydrogen bonds. A bulkier pendant may force the polymer chain to take a more twist conformation but hamper hydrogen-bond formation, while the opposite is true for a smaller pendant. The L-leucine pendants in PPA-Le and PPA-L are bulkier than the L-alanine units in PPA-Ae and PPA-A. The L-leucine-containing polymers show lower $[\alpha]_D^{20}$ and $[\theta]$ values than their congeners with L-alanine pendants measured under the same solvents. This indicates that hydrogen bonding plays a crucial role in stabilizing the helicity of the PPAs carrying amino acid pendants. The smaller alanine pendants in PPA-Ae and PPA-A chains exert little interference on the formation of intra- and interstrand hydrogen bonds, which stabilizes the helical conformations of polymer chains induced by the chiral amino acid pendants.

Supramolecular Assembling. In nature, the helical chains of biopolymers self-fold into high-order structures via cooperative association processes.[20] Can our polymers self-organize into hierarchical structures as the natural biopolymers do? To answer this question, we studied the assembling processes and aggregate morphologies of our polymers. A simple evaporation process was employed in our study. A tiny drop (a few microliters in volume) of a polymer solution was placed on a clean substrate, and the solvent was allowed to evaporate naturally under ambient conditions.

Natural evaporation of 5 μL of a dilute methanol solution of PPA-Ae (43.2 μM) on freshly cleaved mica affords helical

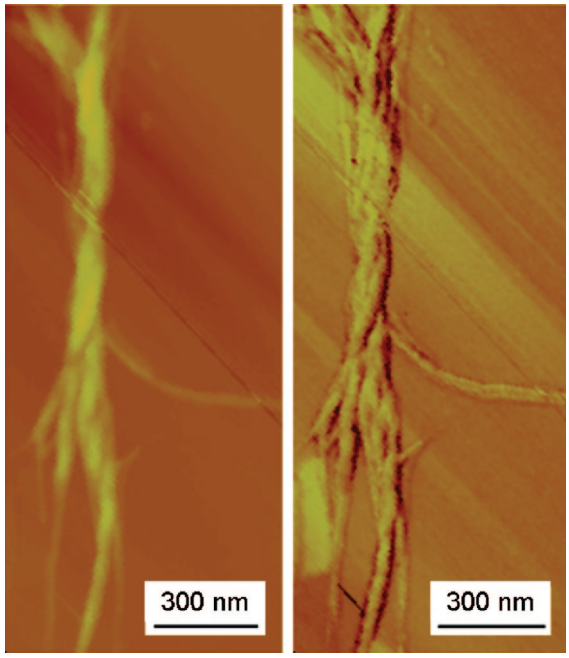

Figure 7. AFM height (left) and phase (right) images of multistranded right-handed helixes formed upon natural evaporation of a dilute methanol solution of PPA-Ae (43.2 μM; sample from Table 1, no. 11) on a newly cleaved mica.

cables with right-handed twists (Figure 7). The heights and widths of the helical fibrils are, on average, ~12 and ~64 nm, respectively, and their lengths can be very long (up to several micrometers). These scales are much bigger than the dimension of a single polymer chain, indicating that the helical ropes are the assemblies of multiple strands of the polymer chains. Owing to the strong solvating power of methanol, the PPA-Ae chains may take an extended conformation in the solution. Accompanying the solvent evaporation, the individual helical polymer chains may intertwine via noncovalent interactions such as interchain hydrogen bonding to form spirally twisting fibrils.[21] While the side-by-side hydrogen bonding of the polymer chains yields thick nanofibers, their aggregation in head-to-tail fashion extends the lengths of the cables.

It is truly amazing that such a well-organized morphological structure is formed almost spontaneously and instantly, taking into account that the tiny amount of methanol solvent needs only a split second to evaporate in open air at ambient temperature. Because of its high molecular weight (M_w ~ 426 000), PPA-Ae should have started to aggregate at an even earlier stage well before all the solvent molecules evaporate. Thus, like those of the natural biopolymers, the assembling of the helical chains of PPA-Ae should also be highly cooperative.[19,20]

We prepared a dilute methanol solution (10.3 μM) of PPA-Ae with the hope of seeing elementary processes toward the formation of the helical cable. Natural evaporation of this solution affords helical ribbons (Figure 8A). Thin layers of polymer films are also formed. The parts of the mica covered by the polymer films are in lighter color, allowing easy identification of the boundaries between covered and uncovered parts. The films are not smooth and have many holes because they are extremely thin. Careful inspections reveal that they are titled with the helical ribbons at the edges. These morphologies suggest the following pathway for the chain folding: rolling up of the polymer films gives the helical ribbons, further association of which in different multiplicities (doublet, triplet, quadruplet, etc.) affords multistranded cable. Because the polymer films roll up in a statistic fashion, ribbons of varying sizes are formed. Even within a single ribbon, its diameter and pitch can be different: the ribbon becomes thicker and the pitch becomes longer when moving from spot "a" to spot "c" in Figure 8C.

Similarly, polymer films with helical ribbons are evolved upon natural evaporation of a dilute THF solution of PPA-Ae (Figure 9). Unlike those formed from the evaporation of the methanol solution, the helical ribbons observed here are left-handed and twisting spirally. Some of them are coiling around to form ring-shaped or cagelike morphologies. The atomic force microscope (AFM) images appear to be visual representations of the CD spectral data given in Figure 5. PPA-Ae exhibits stronger Cotton effect in THF than in methanol; accordingly, better-ordered hierarchical structures of superhelical ribbons are formed via the evaporation-induced supramolecular self-assembling processes of the THF solution.

Characterization by transmission electron microscope (TEM) offers information on not only external but also internal structure of the assembling morphologies. Figure 10 shows the TEM micrograph of the helical ribbons of PPA-Ae formed on a carbon-coated copper grid. The contrast between the edges and the interiors of the ribbons indicates that the ribbons are empty nanotubes. The tubes entwine around each other to give twisted hollow cables reminiscent of neuron dendrites. Similar morphology has been observed in a polyacetylene containing L-isoleucine moieties.[2b]

The morphology obtained from natural evaporation of a chloroform solution of PPA-Ae with a similar concentration (43.2 μM) is distinctly different. Instead of helical cables, oval eggs or spherical vesicles are formed (Figure 11A). This difference is, however, not totally unexpected. Unlike methanol and THF, chloroform is a poor solvent of the amino acid pendants. The amphiphilic polymer chains may form micelle-like structures with the L-alanine methyl ester pendants located in the cores and the PPA backbones positioned outward on the shells. During the solvent evaporation, the micelles may grow in size and stick together via intermicellar hydrogen bonding to form large micelles to minimize the interfacial surface areas.[22] Similarly, the large micelles can further merge into pearl-like nanospheres, again with the aid of intershell hydrogen bonding. When a chloroform solution with a relatively high concentration (6.5 μM) is used, a piece of nice mesoporous film is formed (Figure 11B), thanks to the excellent film-forming ability of this high molecular weight polymer. Spreading a tiny drop of the polymer solution on a carbon-coated copper grid affords a thin film with many concentric rings of varying diameters (Figure 11C).

The insolubility of PPA-A in nonpolar solvents with low boiling points hampered our investigation on its self-assembling processes. Figure 12 shows a pigtail-like fibrous morphology observed upon natural evaporation of a methanol solution of PPA-A on a newly cleaved mica. Unlike those shown in Figure 7, the helixes observed here are looser with larger pitches. Self-weaving of the helical PPA-A chains into the thick, long fibrillar cables is believed to be aided by the interchain hydrogen bonding. Formation of hydrogen bonds between the carboxylic protons of L-alanine pendants of the polymer and the hydroxyl groups of the solvent molecules, however, breaks such physical forces, resulting in a partial unravel of the twisting ropes.

Biological Compatibility. Decorating the polyacetylene backbones with the pendants of naturally occurring building blocks may impart biocompatibility to the conjugated polymers. In our previous study, we have found that the sugar-decorated PPAs are cytophilic and can stimulate the growth of living cells.[2b,23] Would PPA-A, a polyacetylene decorated by L-alanine pendants, be biocompatible? To address this issue, we investigated its cytotoxicity to living HeLa cells. The cells were subcultured onto the microtiter plates precoated with the PPA-A

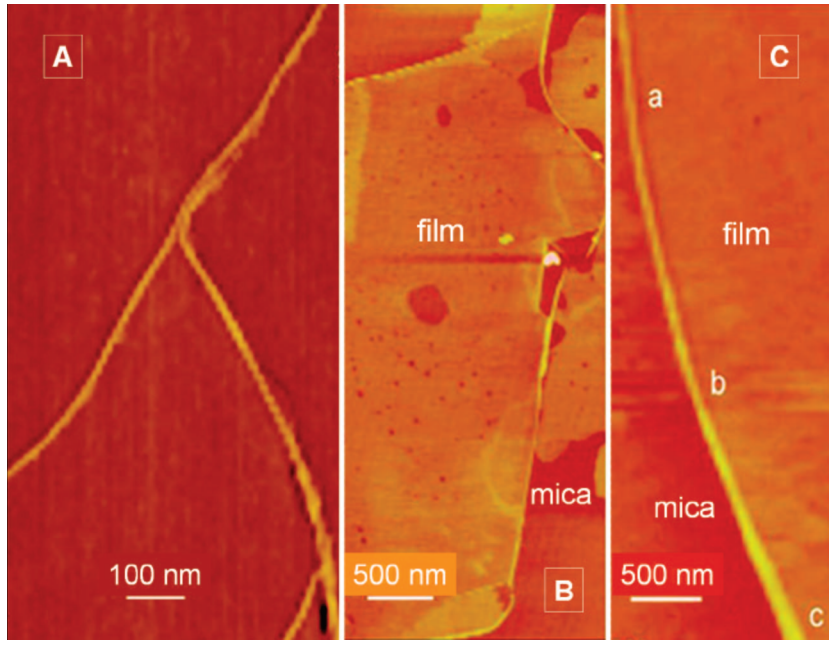

Figure 8. (A) AFM height image of right-handed helical ribbons formed upon natural evaporation of a methanol solution of PPA-Ae (~2.5 μg/mL) on a newly cleaved mica under ambient conditions. (B) Formation of helical ribbons by rolling up of polymer films from the edges; the parts of the mica substrates covered and uncovered by the polymer films are in lighter and darker colors, respectively. (C) Different extent of rolling of a polymer film at its edge gives a helical nanofiber with different diameters and pitches (labeled by a, b, and c).

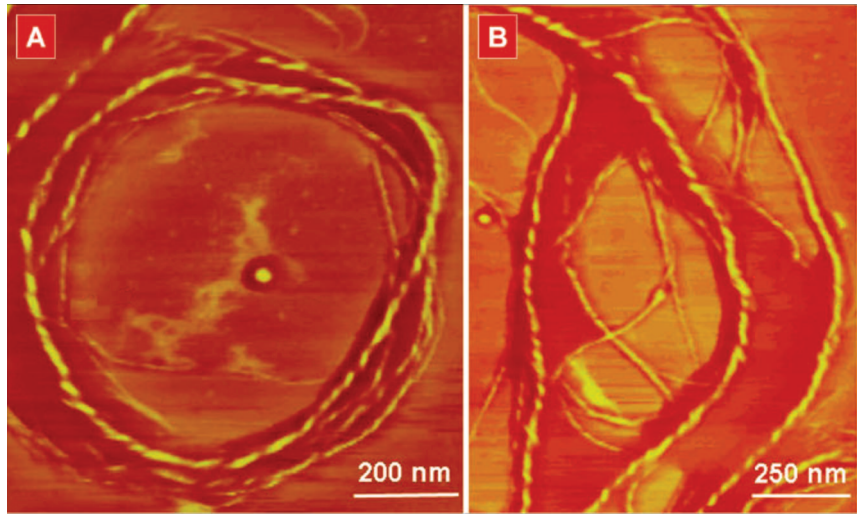

Figure 9. Phase images of superhelical ribbons with left-handed twists formed upon natural evaporation of a THF solution of PPA-Ae (~2.5 μg/mL; sample taken from Table 1, no. 11). Thin films are formed along with the helical ribbons. The substrate covered by the polymer film is in lighter color, while the bare mica is in darker color.

films, and the adhesion and growth of the cells were observed on an optical microscope. After incubation for 1 day, the cells are found to adhere to, and grow on, the plates as they do in the control experiment, in which the plates without the polymer coatings are used (Figure 13). The polymer exhibits no toxicity to the cells; in other words, PPA-A is biocompatible. Even when the polymer coating density is as high as ~22 mg/cm^2, no dead cells are found throughout the experiment, demonstrative of excellent cytocompatibility of the polymer.

Concluding Remarks

In this work, we melded a proteinogenic amino acid, L-alanine, with a synthetic conjugated polymer, polyacetylene, at molecular level through covalent bonding and generated amphiphilic polymer hybrids that possess helical chirality and are capable of self-assembling. The Ala-PPA molecular hybrids with high molecular weights and stereoregularities were synthesized in high yields by the rhodium-catalyzed polymerization. The resultant polyester was converted into its corresponding polyacid by selective hydrolysis without harming the amide functional group. The polymers are thermally stable ($T_d \geq 270$ °C) and undergo irreversible *Z*-to-*E* chain isomerization when heated to ~180−250 °C. The polymers show strong CD bands in the long wavelength region, proving that the chiral amino acid pendants have induced the polyacetylene strands to rotate in a helical screw sense. In comparison to the bulkier L-leucine pendants, the smaller L-alanine pendants exhibit higher helical induction power due to the stronger stabilization effect of the hydrogen bonds in the latter system. The chain amphiphilicity and hydrogen-bonding capability encoded in the primary structure confer a rich structural hierarchy on the hybrid polymers, enabling them to self-assemble cooperatively into

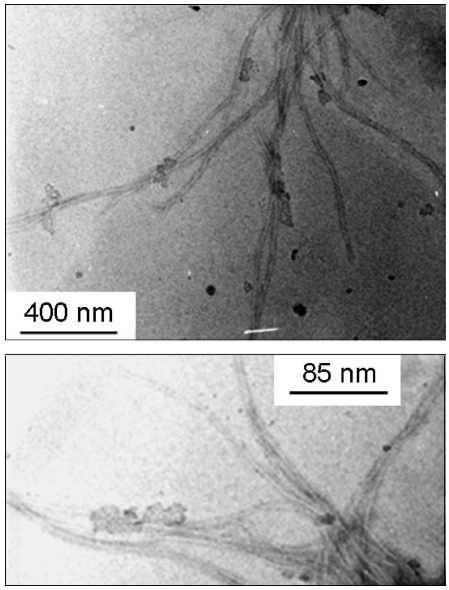

Figure 10. Helical nanotubes formed upon natural evaporation of a methanol solution of PPA-Ae (43.2 μM; sample from Table 1, no. 11) on a carbon-coated copper grid.

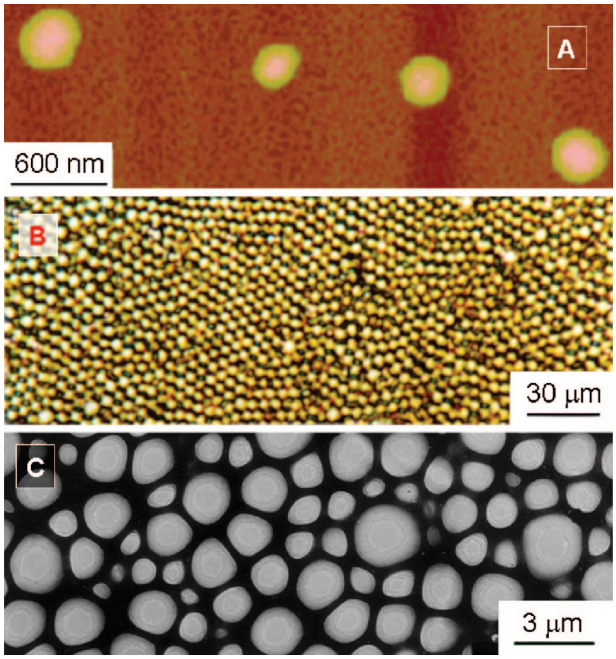

Figure 11. (A) AFM image of nanospheres formed upon natural evaporation of a dilute chloroform solution of PPA-Ae (43.2 μM; sample from Table 1, no. 11) on a newly cleaved mica. (B) Polarized optical microscope (POM) and (C) TEM images of porous films formed by natural evaporation of a "concentrated" chloroform solution of PPA-Ae (6.5 mM) on (B) glass slide and (C) carbon-coated copper grid.

supramolecular morphologies such as twisting cables, spiral ribbons, spherical vesicles, and helical nanotubes. The chiral polymers are biocompatible and exert no cytotoxic effects on the growth of living cells.

Unlike copolymers, homopolymers has generally been believed to be difficult to self-assemble into well-defined morphological structures.[24] Our polymers, being homopolymers notwithstanding, can spontaneously form supramolecular assemblies of defined architectures. This clearly demonstrates that unnatural polymers with rationally designed molecular structures can be used as architectural units for nanostructure morphofabrication. Unlike "conventional" vinyl polymers, polyacetylenes are consisted of alternating double bonds, some of which are highly photoconductive.[25] Coupled with their easy preparation, our polymers promise innovative technological applications in biotechnology systems as artificial nerves, anisotropic molecular wires, and photosynthesis devices.

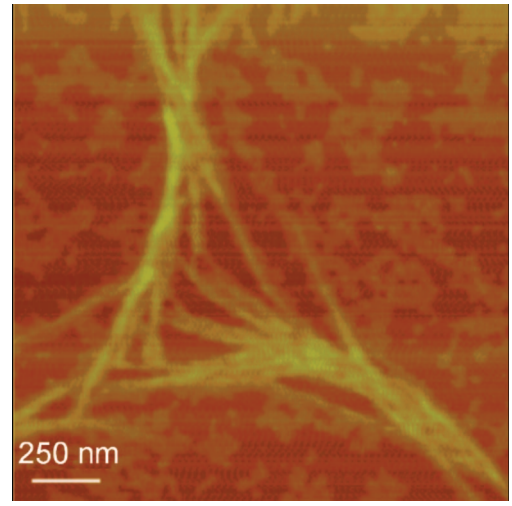

Figure 12. AFM height image of pigtail-like nanofibers formed upon natural evaporation of a methanol solution of PPA-A (46.0 μM) on a newly cleaved mica.

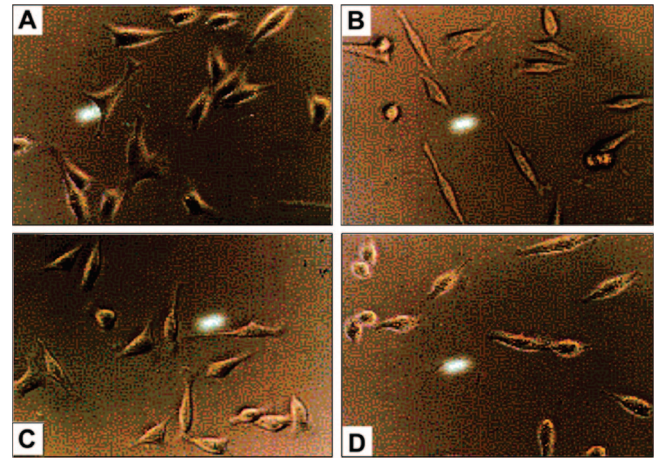

Figure 13. Adhesion of living HeLa cells to the microtiter plates precoated with different amounts of PPA-A (μg/cm^2): (A) 0 (control), (B) 10.53, (C) 15.78, and (D) 22.24. Incubation time: 1 day.

Experimental Section

Materials. Dioxane, toluene, and THF were purchased from Aldrich, dried over 4 Å molecular sieves, and distilled under nitrogen from sodium benzophenone ketyl immediately prior to use. DCM (Laboratory-Scan) and acetone (RdH) were distilled under nitrogen over calcium hydride. TEA and pyridine (RdH) were distilled under normal pressure and dried over KOH. L-Alanine methyl ester hydrochloride (Sigma), tungsten(VI) chloride, tetraphenyltin (Aldrich), molybdenum(V) chloride (Acros), potassium hydroxide, and methanol (both RdH) were used as received without further purification. 4-Ethynylbenzoyl chloride (**1**) was prepared from 4-ethynylbenzoic acid.[3] The organorhodium complexes were prepared according to published procedures.[6f]

Instrumentation. IR spectra were recorded on a Perkin-Elmer 16 PC FT-IR spectrometer. ^{1}H and ^{13}C NMR spectra were measured on a Bruker ARX 300 NMR spectrometer or a JEOL 400 NMR spectrometer using chloroform-*d*, acetone-d_6, or methanol-d_4 as solvents. Tetramethylsilane (TMS), chloroform, acetone, or methanol was used as internal references for the NMR analysis. UV

spectra were recorded on a Milton Roy Spectronic 3000 Array spectrophotometer, and molar absorptivities (ε) of the polymers were calculated on the basis of their repeat units. MALDI-TOF high-resolution mass (HRMS) spectra were recorded on a GCT Premier CAB048 mass spectrometer with methane as carrier gas. Molecular weights (M_w and M_n) and polydispersities (M_w/M_n) of the polymers were estimated by GPC using a Waters Associates liquid chromatograph equipped with a Waters 510 HPLC pump, a Pheodyne 7725i injector with a stand kit, a set of Styragel columns (HT3, HT4, and HT6; molecular weight range 10^2-10^7), a column temperature controller, a Waters 486 wavelength-tunable UV detector, a Waters 410 differential refractometer, and a system DMM/scanner with an 8-channel scanner option. All the polymer solutions were prepared in THF (ca. 2 mg/mL) and filtered through 0.45 mm PTFE syringe-type filters before being injected into the GPC system. THF was used as eluent at a flow rate of 1.0 mL/min. The column temperature was maintained at 40 °C, and the working wavelength of the UV detector was set at 254 nm. A set of monodisperse polystyrene standards (Waters) was used for calibration purposes.

TGA of the polymers was performed on a Perkin-Elmer TGA 7 under nitrogen at a heating rate of 20 °C/min. DSC thermograms of the polymers were recorded on a Setaram DSC 92 under nitrogen at a scanning rate of 10 °C/min. $[\alpha]_D^{20}$ values of the polymers were measured on a Perkin-Elmer 241 polarimeter at 20 °C using a beam of plane-polarized light of the D line of a sodium lamp (589.3 nm) as the monochromatic source. CD measurements were conducted on a Jasco J-720 spectropolarimeter using 1 mm quartz curette at room temperature. The spectra were recorded with a step resolution of 0.2 nm, a scan speed of 50 nm/min, a sensitivity of 100 mdeg, and a response time of 0.5 s. Each spectrum was the average of 5−10 scans. The concentrations of the polymers were calculated on the basis of their repeat units.

AFM images were obtained on a Digital Instrument Nano IIIa microscope of Digital Instrument Co. (Santa Barbara, CA) in tapping mode using hard silicon tip. The images were collected with a maximum number of pixels (512 × 512) and were only processed by flattening. TEM images were recorded on a Philip CM20 TEM operating at 200 kV. Photomicrographs were taken under bright field on an Olympus BX 60 POM using a polarized light source.

Monomer Preparation. The L-alanine−phenylacetylene adduct, 4-ethynylbenzoyl-L-alanine methyl ester (PA-Ae), was prepared by amidation of 4-ethynylbenzoyl chloride (**1**) with L-alanine methyl ester hydrochloride (**2**; Scheme 1). Typical experimental procedures for the synthesis of the monomer are given below.

Into a 100 mL round-bottom flask were added 0.85 g (6.1 mmol) of **2** and 3 mL of pyridine in 10 mL of DCM under nitrogen. The flask was cooled to 0 °C, into which a solution of **1** (1.00 g, 6.1 mmol) in 10 mL of DCM was slowly injected. After stirring for 24 h at room temperature, the solution was diluted with 100 mL of DCM and washed twice with dilute aqueous hydrochloric acid and once with water. The organic layer was dried over 5 g of magnesium sulfate. After filtration and solvent evaporation, the crude product was purified on a silica gel column using chloroform/acetone (15:1 by volume) mixture as eluent. A white solid was obtained in 68.1% yield (0.96 g). IR (KBr), ν (cm^{-1}): 2104 (C≡C stretching), 1738 (C═O stretching in CO_2CH_3), 1640 (C═O stretching in CONH). ^1H NMR (300 MHz, $CDCl_3$), δ (TMS, ppm): 7.8 (m, 2H, aromatic protons ortho to C═O), 7.6 (m, 2H, aromatic protons meta to C═O), 6.8 (d, 1H, NH), 4.8 (m, 1H, NHC*H*), 3.8 (s, 3H, CO_2CH_3), 3.2 (s, 1H, ≡CH), 1.5 (m, 3H, CH_3). ^{13}C NMR (75 MHz, $CDCl_3$), δ (TMS, ppm): 173.6 (CO_2), 166.0 (CONH), 133.8 (aromatic carbon attached to C═O), 132.3 (aromatic carbons meta to C═O), 127.1 (aromatic carbons ortho to C═O), 125.6 (aromatic carbon para to C═O), 82.7 (Ph*C*≡), 79.6 (HC≡), 52.6 (CO_2CH_3), 48.5 (NHCH), 18.5 (CH_3). HRMS (MALDI-TOF): *m*/*z* 232.0974 [$(M + H)^+$, calcd 232.0929].

Polymer Synthesis. All the polymerization reactions and manipulations were carried out under dry nitrogen using either an inert-atmosphere glovebox (Vacuum Atmospheres) or Schlenk techniques in vacuum-line systems except for the purification of the polymers, which was done in a fume hood in open air. Typical experimental procedures for the synthesis of poly[4-ethynylbenzoyl-L-alanine methyl ester] (PPA-Ae) from the polymerization of PA-Ae catalyzed by $[Rh(nbd)Cl]_2$ in a THF/TEA mixture are given below.

Into a 20 mL Schlenk tube with sidearm was added 0.2 mmol of PA-Ae. The tube was evacuated under vacuum and then flushed with dry nitrogen three times through the sidearm. THF (1 mL) was injected into the tube to dissolve the monomer. The catalyst solution was prepared in another tube by dissolving 0.01 mmol of $[Rh(nbd)Cl]_2$ in 1 mL of THF with 1 drop of TEA, which was transferred to the monomer solution using a hypodermic syringe. The reaction mixture was stirred at room temperature under nitrogen for 24 h. The mixture was then diluted with 2 mL of THF and added dropwise to a mixture of acetone/diethyl ether (150 mL) under stirring. The precipitate was filtered and dried in a vacuum oven at room temperature to a constant weight. A yellowish powder was obtained in 83.0% yield. M_w 426 000; M_w/M_n 5.11 (GPC, polystyrene calibration). IR (KBr), ν (cm^{-1}): 1741 (C═O stretching in CO_2CH_3), 1644 (C═O stretching in CONH). ^1H NMR (300 MHz, acetone-d_6), δ (acetone-d_6, ppm): 8.0 (NH), 7.4 (aromatic protons ortho to C═O), 6.7 (aromatic protons meta to C═O), 5.9 (*Z* olefin proton), 4.5 (NHC*H*), 3.6 (CO_2CH_3), 1.4 (CH_3). ^{13}C NMR (75 MHz, acetone-d_6), δ (acetone-d_6, ppm): 174.1 (CO_2), 167.5 (CONH), 145.8 (=*C*Ph), 139.4 (aromatic carbon para to C═O), 134.0 (aromatic carbon attached to C═O), 128.4 (aromatic carbons ortho to C═O, HC═, and aromatic carbons meta to C═O), 52.4 (CO_2CH_3), 49.5 (NHCH), 17.5 (CH_3). UV (MeOH, 1.60×10^{-4} mol/L), λ_{max} (nm)/ε_{max} (mol^{-1} L cm^{-1}): 273/9.09×10^3, 395/3.43×10^3.

Ester Hydrolysis. Polyacid poly[4-ethynylbenzoyl-L-alanine] (PPA-A) was obtained by hydrolysis of PPA-Ae under basic conditions (Scheme 1). Into a 50 mL round-bottom flask equipped with a stirrer bar were added 178 mg (0.77 mmol) of PPA-Ae (sample from Table 1, no. 11) and 2 g (35.6 mmol) of KOH in 20 mL of methanol. After stirring at room temperature for 1 h, the solution was poured into a dilute aqueous solution of hydrochloric acid. The precipitate was collected by filtration and dried under vacuum. A yellowish solid with a *Z* content of 75.9% was obtained in 95.7% yield (0.16 g). IR (KBr), ν (cm^{-1}): 1638 (C═O stretching in CONH). ^1H NMR (400 MHz, CD_3OD), δ (TMS, ppm): 7.6 (aromatic protons ortho to C═O), 6.8 (aromatic protons meta to C═O), 5.9 (*Z* olefin proton), 4.5 (NHC*H*), 1.5 (CH_3). ^{13}C NMR (100 MHz, CD_3OD), δ (TMS, ppm): 176.1 (CO_2), 169.0 (CONH), 146.5 (=*C*Ph), 140.0 (aromatic carbon para to C═O), 133.6 (aromatic carbon attached to C═O), 128.5 (aromatic carbons ortho to C═O, HC═, and aromatic carbons meta to C═O), 50.0 (NHCH), 17.5 (CH_3). UV (MeOH, 1.61×10^{-4} mol/L), λ_{max} (nm)/ε_{max} (mol^{-1} L cm^{-1}): 273/8.70×10^3, 395/2.59×10^3.

Supramolecular Self-Assembling. The polymer chains were allowed to self-assemble under ambient conditions (1 atm, ∼20−22 °C, ∼55−70% relative humidity). A concentrated stock solution of PPA-Ae in methanol, THF, or chloroform was initially prepared, which was then diluted with methanol, THF, or chloroform to desire concentrations (∼2.5−43.2 μM). Tiny drops (∼3−30 μL) of the polymer solutions on substrates were allowed to naturally evaporate without exercising any external engineering controls to ensure that the polymer chains were self-assembled without perturbations under the particular sets of environmental conditions.

Cell Culture. The biological effect of PPA-A was studied using living HeLa cells in a clean room. The cells were cultured in Dulbecco's modified Eagle's medium (DMEM; Gibco) supplemented with 10% fetal bovine serum (Gibco), 1% penicillin/streptomycin/amphotericin (PSA) antibiotic mixture (Gibco), and 1% L-glutamine (Gibco) at 37 °C in a 5% CO_2 atmosphere. The living cells were harvested at 80−90% confluence and were subcultured onto 96-well microtiter plates precoated with the PPA-A films at a concentration of 800−900 cells/well. The polymer coatings were prepared by natural evaporation of appropriate amounts of methanol solution of the polymer (0.01 mg/mL) in a fume hood. The wells without polymer coatings were used as

controls. The adhesion and growth of the cells were observed under an optical microscope (Olympus).

Acknowledgment. The work reported in this paper was partially supported by the Research Grants Council of Hong Kong (602707, 602706, and HKU2/05C), the Ministry of Science & Technology of China (2002CB613401), and the National Natural Science Foundation of China (20634020). B.Z.T. thanks the support from the Cao Guangbiao Foundation of Zhejiang University.

References and Notes

(1) (a) *Mechanisms of Protein Folding*, 2nd ed.; Pain, R. H., Ed.; Oxford University Press: Oxford, 2000. (b) *Protein Flexibility and Folding*; Kuhn, L. A., Thorpe, M. F., Eds.; Elsevier: Amsterdam, 2001.

(2) (a) Lam, J. W. Y.; Tang, B. Z. *Acc. Chem. Res.* **2005**, *38*, 745. (b) Cheuk, K. K. L.; Li, B. S.; Tang, B. Z. *Curr. Trends. Polym. Sci.* **2002**, *7*, 41. (c) Tang, B. Z. *Polym. News* **2001**, *26*, 262. (d) Lai, L. M.; Lam, J. W. Y.; Tang, B. Z. *J. Polym. Sci., Part A: Polym. Chem.* **2006**, *44*, 6190. (e) Lai, L. M.; Lam, J. W. Y.; Qin, A.; Dong, Y.; Tang, B. Z. *J. Phys. Chem. B* **2006**, *110*, 11128. (f) Cheuk, K. K. L.; Lam, J. W.Y.; Lai, L. M.; Dong, Y. P.; Tang, B. Z. *Macromolecules* **2003**, *36*, 9572.

(3) Cheuk, K. K. L.; Lam, J. W. Y.; Chen, J.; Lai, L. M.; Tang, B. Z. *Macromolecules* **2003**, *36*, 5947.

(4) (a) Li, B.; Kang, S.; Cheuk, K. K. L.; Wan, L.; Ling, L.; Bai, C.; Tang, B. Z. *Langmuir* **2004**, *20*, 7589. (b) Li, B.; Cheuk, K. K. L.; Yang, D.; Lam, J. W. Y.; Wan, L.; Bai, C.; Tang, B. Z. *Macromolecules* **2003**, *36*, 5447. (c) Li, B.; Cheuk, K. K. L.; Ling, L.; Chen, J.; Xiao, X.; Bai, C.; Tang, B. Z. *Macromolecules* **2003**, *36*, 77. (d) Li, B.; Cheuk, K. K. L.; Salhi, F.; La, J. W. Y.; Cha, J. A. K.; Xiao, X.; Bai, C.; Tang, B. Z. *Nano Lett.* **2001**, *1*, 323. (e) Salhi, F.; Cheuk, K. L.; Lam, J. W. Y.; Cha, J. A. K.; Li, G.; Li, B.; Luo, J.; Chen, J.; Tang, B. Z. *J. Nanosci. Nanotechnol.* **2001**, *1*, 137.

(5) (a) Masuda, T.; Higashimura, T. *Adv. Polym. Sci.* **1987**, *81*, 121. (b) Lam, J. W. Y.; Kong, X.; Dong, Y. P.; Cheuk, K. K. L.; Xu, K.; Tang, B. Z. *Macromolecules* **2000**, *33*, 5027. (c) Reddinger, J. L.; Reynolds, J. R. *Adv. Polym. Sci.* **1999**, *145*, 57. (d) Li, C. H.; Li, Y. L. *Macromol. Chem. Phys.* **2008**, *209*, 000DOI 10.1002/macp.200800049.

(6) (a) Masuda, T. *J. Polym. Sci., Part A: Polym. Chem.* **2007**, *45*, 165. (b) Masuda, T.; Sanda, F. In *Handbook of Metathesis*; Grubbs, H., Ed.; VCH: Weinheim, 2003; Vol. *3*, Chapter 11. (c) Sedlacek, J.; Vohlidal, J. *Collect. Czech. Chem. Commun.* **2003**, *68*, 1745. (d) Yin, S.; Xu, H.; Su, X.; Gao, Y.; Song, Y.; Lam, J. W. Y.; Tang, B. Z.; Shi, W. *Polymer* **2005**, *46*, 10592. (e) Tang, B. Z.; Kong, X.; Wan, X.; Feng, X.-D. *Macromolecules* **1997**, *30*, 5620. (f) Tang, B. Z.; Poon, W. H.; Leung, S. M.; Leung, W. H.; Peng, H. *Macromolecules* **1997**, *30*, 2209.

(7) Silverstein, R. M.; Bassler, G. C.; Morrill, T. C. *Spectrometric Identification of Organic Compounds*, 5th ed.; Wiley: New York, 1991.

(8) Percec, V.; Rudick, J. G.; Peterca, M.; Wagner, M.; Obata, M.; Mitchell, C. M.; Cho, W. D.; Balagurusamy, V. S. K.; Heiney, P. A. *J. Am. Chem. Soc.* **2005**, *127*, 15257.

(9) (a) Lam, J. W. Y.; Dong, Y.; Cheuk, K. K. L.; Luo, J.; Xie, Z.; Kwok, H. S.; Mo, Z.; Tang, B. Z. *Macromolecules* **2002**, *35*, 1229. (b) Tang, B. Z.; Kong, X.; Wan, X.; Peng, H.; Lam, W. Y.; Feng, X.-D.; Kwok, H. S. *Macromolecules* **1998**, *31*, 2419. (c) Dumitrescu, S.; Percec, V.; Simionescu, C. I. *J. Polym. Sci., Polym. Chem. Ed.* **1977**, *15*, 2893.

(10) (a) Yang, W.; Tabata, M.; Kobayashi, S.; Yokota, K.; Shimizu, A. *Polym. J.* **1991**, *23*, 1135. (b) Balcar, H.; Sedlacek, J.; Vohlidal, J.; Zednik, J.; Blechta, V. *Macromol. Chem. Phys.* **1999**, *200*, 2591. (c) Schenning, A. P. H. J.; Fransen, M.; Meijer, E. W. *Macromol. Rapid Commun.* **2002**, *23*, 266. (d) Russo, M. V.; Iucci, G.; Furlani, A.; Camus, A.; Marsich, N. *Appl. Organomet. Chem.* **1992**, *6*, 517.

(11) (a) Percec, V.; Rinalki, P. L. *Polym. Bull.* **1983**, *9*, 548. (b) Furlani, A.; Napoletano, C.; Russo, M. V.; Feast, W. J. *Polym. Bull.* **1986**, *16*, 311.

(12) Robertson, J. *Protecting Group Chemistry*; Oxford University Press: New York, 2000.

(13) (a) Masuda, T.; Tang, B. Z.; Higashimura, T. *Macromolecules* **1985**, *18*, 2369. (b) Vohlidal, J.; Kabatek, Z.; Pacovska, M.; Sedlacek, J.; Grubisicgallot, Z. *Collect. Czech. Chem. Commun.* **1996**, *61*, 120.

(14) (a) Masuda, T.; Tang, B. Z.; Tanaka, T.; Higashimura, T. *Macromolecules* **1986**, *19*, 1459. (b) Seki, H.; Tang, B. Z.; Tanaka, A.; Masuda, T. *Polymer* **1994**, *35*, 3456.

(15) (a) Tang, B. Z.; Kotera, N. *Macromolecules* **1989**, *22*, 4388. (b) Lam, J. W. Y.; Dong, Y.; Cheuk, K. K. L.; Tang, B. Z. *Macromolecules* **2003**, *36*, 7927. (c) Lam, J. W. Y.; Dong, Y. P.; Cheuk, K. K. L.; Law, C. C. W.; Lai, L. M.; Tang, B. Z. *Macromolecules* **2004**, *37*, 6695.

(16) (a) Mayer, S.; Zentel, R. *Prog. Polym. Sci.* **2001**, *26*, 1973. (b) Percec, V.; Obata, M.; Rudick, J. G.; De, B. B.; Glodde, M.; Bera, T. K.; Magonov, S. N.; Balagurusamy, V. S. K.; Heiney, P. A. *J. Polym. Sci., Part A: Polym. Chem.* **2002**, *40*, 3509. (c) Yashima, E. *Anal. Sci.* **2002**, *18*, 3. (d) Teramoto, A. *Prog. Polym. Sci.* **2001**, *26*, 667.

(17) (a) Akagi, K.; Guo, S.; Mori, T.; Goh, M.; Piao, G.; Kyotani, M. *J. Am. Chem. Soc.* **2005**, *127*, 14647. (b) Fukushima, T.; Takachi, K.; Tsuchihara, K. *Macromolecules* **2006**, *39*, 3103. (c) Iwasaki, T.; Nishide, H. *Curr. Org. Chem.* **2005**, *9*, 1665. (d) Zhao, H. C.; Sanda, F.; Masuda, T. *J. Polym. Sci., Part A: Polym. Chem.* **2005**, *43*, 5168. (e) Gal, Y. S.; Lim, K. T.; Shim, S. Y.; Kim, S. Y. H.; Koh, K.; Jang, S. H.; Jin, S. H. *Synth. Met.* **2005**, *154*, 169. (f) Kang, S. W.; Jin, S. H.; Chien, L. C.; Sprunt, S. *Adv. Funct. Mater.* **2004**, *14*, 329.

(18) *Circular Dichroism: Principles and Applications*; Nakanishi, K., Berova, N., Woody, R. W., Eds.; Wiley-VCH: New York, 2000.

(19) (a) Brizard, A.; Oda, R.; Huc, I. *Top. Curr. Chem.* **2005**, *256*, 167. (b) Fleishman, S. J.; Unger, V. M.; Ben-Tal, N. *Trends Biochem. Sci.* **2006**, *31*, 106. (c) Zubay, G. L. *Biochemistry*, 4th ed.; Wm. C. Brown Publishers: Boston, MA, 1998; Chapters 5 and 8.

(20) Liss, A. R. In *Self-Assembling Architecture*; Varner, J. E., Ed.; New York, 1988.

(21) Brutschy, B.; Hobza, P. *Chem. Rev.* **2000**, *100*, 3861.

(22) Moroi, Y. *Micelles: Theoretical and Applied Aspects*; Plenum Press: New York, 1992.

(23) Cheuk, K. K. L.; Lam, J. W. Y.; Li, B. S.; Xie, Y.; Tang, B. Z. *Macromolecules* **2007**, *40*, 2633.

(24) Yu, S. M.; Soto, C. M.; Tirrell, D. A. *J. Am. Chem. Soc.* **2000**, *122*, 6552.

(25) (a) Tang, B. Z.; Chen, H. Z.; Xu, R. S.; Lam, J. W. Y.; Cheuk, K. K. L.; Wong, H. N. C.; Wang, M. *Chem. Mater.* **2000**, *12*, 213. (b) Vohlidal, J.; Sedlacek, J.; Patev, N.; Lavastre, O.; Dixneuf, P. H.; Cabioch, S.; Balcar, H.; Pfleger, J.; Blechta, V. *Macromolecules* **1999**, *32*, 6439.

MA800976E